

# Quantized Topological Charges of Ferroelectric Skyrmions in Two-Dimensional Multiferroic Materials

Zhaosen Liu\*

*College of Physics and Electronic Engineering,  
Hengyang Normal University, Hengyang 421002, China*

## Abstract

In multiferroic materials, the microscopic magnetic and electric textures are strongly correlated with each other by magnetoelectric (ME) coupling. Therefore, topological electric dipole textures, such as ferroelectric (FE) dipole skyrmions and periodic FE dipole crystals, are expected to be induced if ferromagnetic (FM) skyrmions and FM skyrmionic crystals (or lattices so as to be abbreviated as SLs for convenience) can be stabilized. In the present work, a quantum computational approach is utilized to simulate the topological textures of FE SLs in a two-dimensional (2D) multiferroic system. Consequently, we find that, FE SLs can indeed be induced once the FM SLs are formed; each FE skyrmion is an ferroelectric dipolar complex formed around an FM skyrmion; the topological charges of these FE skyrmions are usually quantized to be integers, half integers and multiples of certain fractional values, so that the FE SL coincides precisely with the corresponding FM SL; the topological charge density of each FE SL also forms periodic pattern; and a normally applied electric field is able to change the sizes of FM skyrmions, elevate their formation temperatures, and destroy FM SLs below the critical temperatures as well.

PACS numbers: 75.40.Mg, 75.10.Jm

---

\* Email: liuzhsnj@yahoo.com, zslu@hynu.edu.cn

Keywords: Multiferroic Materials, Ferroelectric Skyrmions, Quantized Topological Charges

## I. INTRODUCTION

Magnetic skyrmions were theoretically predicted by Bogdanov *et. al* as stable magnetic states in chiral magnets [1, 2], and discovered in helimagnetic conductor MnSi about twenty years later [3, 4]. These quasi-particles textures built of topologically protected vortices [5, 6] are mainly caused by Dzyaloshinskii-Moriya interactions (DMI) arising from inversion symmetry breaking [7–11]. Due to their small sizes, topological stability, and greatly reduced electronic currents required to be driven to motion, magnetic skyrmions are believed to be promising candidates in future data storage and racetrack memory, thus have been intensively studied in recent years [12–19].

Magnetic skyrmions in metals can be created, deleted and driven to motion by applied spin electric currents based on the spin transfer torque (STT) mechanism [20–23]. However, the Ohmic heating incurred by the currents are undesirable for electronics, and the STT technique does not work in insulators since electric currents cannot pass through. Fortunately, the magneto-electric coupling that is present in multiferroic insulators, such as  $\text{Cu}_2\text{OSeO}_3$  [24], opens a new way to manipulate magnetic skyrmions by means of electric fields. In these materials, ME coupling arises from the so-called *p-d* hybridization mechanism [24–27], and the electric dipole moments can be expressed in terms of magnetic spins,  $\mathbf{P} = \alpha (S_i^y S_i^z, S_i^z S_i^x, S_i^x S_i^y)$ . Consequently, the topological FM and FE chiral textures are expected to be present simultaneously [24, 28].

Based on above theory, the chiral textures of electric dipoles and dipolar charge density in  $\text{Cu}_2\text{OSeO}_3$  were simulated, by two research groups, within external magnetic and electric fields applied in various directions [24, 25]. The calculated electric dipole textures exhibited regular and distinct topological characters. Therefore, it is of great interest to further study their topological properties.

For this purpose, the FE SLs of a 2D multiferroic material are calculated here by means of a quantum computational approach [29–32], their topological properties are then further analyzed and characterised. Consequently, we find that an FE SL is induced once one FM SL is stabilized; each FE skyrmion is an electric dipole complex formed around an FM skyrmion, and the topological charges of these FE skyrmions are usually quantized to be integers, half integers and multiples of certain fractional values; the topological charge density of every FE SL also forms periodic pattern; and normally applied electric fields are able to change the sizes of FM skyrmions, elevate the formation temperatures of FM SLs, and destroy them below the critical temperatures as well.

## II. THEORETICAL MODEL AND METHOD

The 2D multiferroic material, simplified here as a monolayer, is assumed to be in the  $xy$ -plane. Its Hamiltonian,  $\mathcal{H} = \mathcal{H}_M + \mathcal{H}_{ME}$ , consists of two parts, which are originated from various magnetic interactions and ME coupling respectively. The first part can be written as

$$\mathcal{H}_M = -\frac{1}{2} \sum_{i,j} [\mathcal{J}_{ij} \mathbf{S}_i \cdot \mathbf{S}_j + \mathbf{D}_{ij} \cdot (\mathbf{S}_i \times \mathbf{S}_j)] - \mathbf{H} \cdot \sum_i \mathbf{S}_i - K_A \sum_i (\mathbf{S}_i \cdot \hat{\mathbf{n}})^2, \quad (1)$$

where  $\mathcal{J}_{ij}$ ,  $\mathbf{D}_{ij}$ ,  $K_A$  are the strengths of HE, DM and uniaxial anisotropic (UMA) interactions respectively. While the portion resulting from ME coupling of strength  $\alpha$  can be expressed with

$$\mathcal{H}_{ME} = -\alpha \sum_i \mathbf{P}_i \cdot \mathbf{E}_i = -\frac{\alpha}{2} \sum_i \mathbf{S}_i \begin{pmatrix} 0 & E_i^z & E_i^y \\ E_i^z & 0 & E_i^x \\ E_i^y & E_i^x & 0 \end{pmatrix} \mathbf{S}_i. \quad (2)$$

Since quantum theory is employed, spins appearing in above Hamiltonian are quantum operators [29–32]; the thermal average of every physical observable  $A$  at temperature  $T$  is evaluated with

$$\langle A \rangle = \frac{\text{Tr} [\hat{A} \exp(\beta \mathcal{H}_i)]}{\text{Tr} [\exp(\beta \mathcal{H}_i)]}, \quad (3)$$

where  $\hat{A}$  is the operator of observable  $A$ ,  $\beta = -1/k_B T$ ; and  $[S_\alpha, S_\beta] = i\hbar S_\gamma \epsilon_{\alpha,\beta,\gamma}$  with  $\alpha, \beta, \gamma = x, y, z$ ,  $\epsilon_{\alpha,\beta,\gamma} = 0, \pm 1$ , depending on the order of  $\alpha, \beta$  and  $\gamma$ . In contrast, two arbitrary spin components simply commute in classical physics. Therefore, the two sorts of methods are different from each other. Especially, the uncertainty principle of quantum theory enables quantum computing codes to tunnel through energy barriers much easily, so as to converge to the equilibrium states without the need to manipulate the spins elaborately.

## III. COMPUTATIONAL RESULTS

We have previously simulated the chiral spin textures of a 2D  $\text{FeSi}_{0.5}\text{Co}_{0.5}\text{Si}$ -like FM thin film [29]. With  $D/\mathcal{J}$  assigned to 1.027 and external magnetic fields of strengths  $H \in (0.15, 0.37)$  applied perpendicularly, FM SLs, as shown in Ref.[13], could be reproduced at low temperatures [29]. In the present work, both  $\mathbf{H}$  and  $\mathbf{E}$  are considered to be applied normally to the 2D multiferroic monolayer of the square structure, where every lattice site is occupied by an  $S = 1$  spin,  $\alpha$  is set to 0.2, while  $D/\mathcal{J}$  to the above same value [13, 29] for direct comparison. This  $D/\mathcal{J}$  ratio is very close to that used by Liu *et al.* in their Monte Carlo simulations for another 2D multiferroic system [26].

## A. Effects of Electric Fields on Sizes and Formation Temperatures of Magnetic Skyrmions

Indeed, external electric fields are able to manipulate magnetic skyrmions through the ME coupling as shown in Figure 1, where the skyrmion sizes are changed and formation temperatures of FM SLs elevated by the electric fields that are applied perpendicularly to the  $xy$ -plane.

In Figure 1(a), only an external magnetic field with strength  $H = 0.2$  is exerted, FM SLs are formed below critical temperature  $T_{SL} = 3.15$ , and each skyrmion in these FM SLs occupies  $N_P = 50$  lattice sites in average. While an electric field is also exerted,  $T_{SL}$  is firstly elevated to 3.16 when  $E \in (0.2, 0.5)$ , then to 3.17 as  $E \in (0.6, 0.9)$ . Meanwhile,  $N_P$  is increased from 50 to 60, then to 64.8 in the two  $E$ -field ranges respectively. However, when  $E$  is increased to 1.0, FM SL can only survive in a narrow high temperature interval  $T \in (3.10, 3.17)$ ; below this interval, FM SL is replaced by FM helical crystal (HL) which persists down to very low temperatures. If  $E$  is further increased to 1.2, only FM HL can be observed at low temperatures.

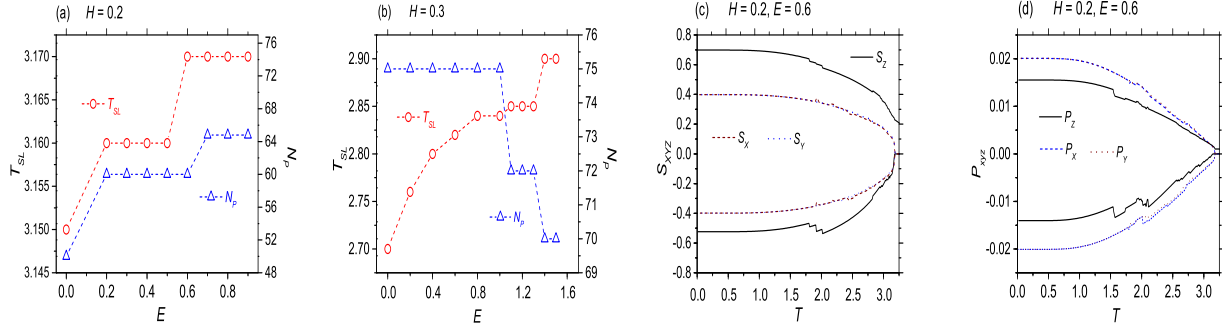


**Figure 1.** Formation temperatures of FM SLs and spins occupied by an FM skyrmion versus normally applied electric field  $E$  when (a,b)  $H = 0.2$ , and  $0.3$  respectively; Thermally averaged values of three components of (c) magnetic spins, and (d) electric polarizations as functions of temperature while  $H = 0.2$  and  $E = 0.6$ , respectively.

In contrast, when  $H = 0.3$ , FM SLs can be stabilized in a wider range  $E \in (0, 1.6)$  as shown in Figure 1(b); and as  $E$  increases,  $T_{SL}$  is elevated considerably from 2.70 to 2.90, but  $N_P$  decreases from 75 to 72 and then to 70 unexpectedly, that is, skyrmion size shrinks in this process.

We have seen that an applied  $E$ -field can strongly affect the microscopic structures of magnetic skyrmions. However, it has much less effects upon the macroscopic magnetic properties. In Figure 1(c),  $E = 0.6$ , the thermally averaged values of  $\langle S_X \rangle$ ,  $\langle S_Y \rangle$  and  $\langle S_Z \rangle$  are plotted. In comparison with those curves obtained free of  $E$ -field interaction which are not presented, the three curves displayed here have actually been slightly modified, but

become a little smoother. That is,  $E$ -fields are able to suppress thermal disturbances and stabilize the FM and FE microscopic structures.

As expected, once an FM SL is induced below the formation temperature  $T_{SL}$ , an FE SL appears immediately due to the ME coupling, and the microscopic configuration of this FE SL can be changed by applied  $E$ -fields for the same reason. Figure 1(d) displays the thermal averaged values of  $\langle P_X \rangle$ ,  $\langle P_Y \rangle$  and  $\langle P_Z \rangle$  versus changing temperature. The two sets of curves that are calculated with the same set of parameters exhibit very similar characters, however  $|\langle P_Z \rangle|$  is much smaller than other two components because of the extremely tiny thickness of the monolayer. Similarly, the  $P_{X,Y,Z}$  curves have only been slightly enhanced in magnitude by the  $E$ -field.

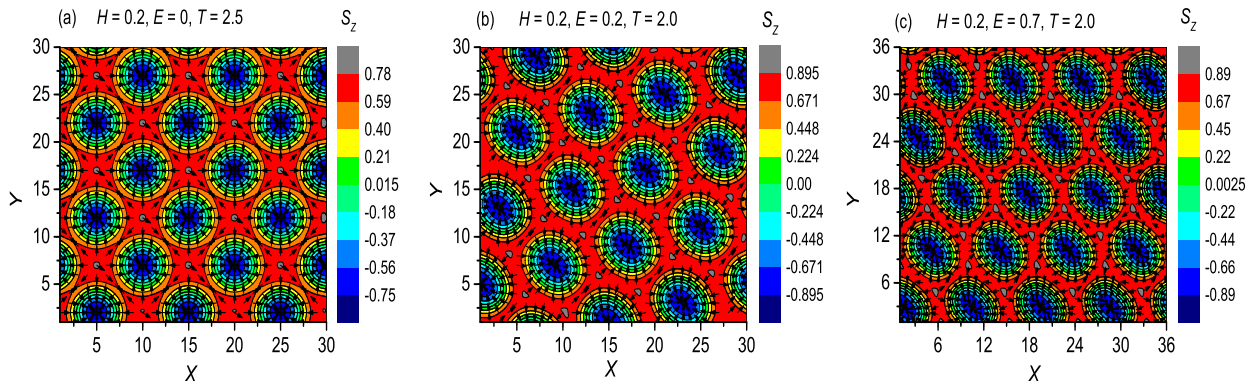


**Figure 2.** FM SLs calculated with  $E$  equal to (a) 0, (b) 0.2, and (c) 0.7 respectively at different temperatures, while  $H = 0.2$  in all of these cases.

The effects of  $E$ -fields upon the microscopic structures of FM SLs are rather pronounced. In Figure 2,  $H$  is fixed to 0.2, while  $E$ -value differs. This gives rise to changed sizes of skyrmions which can be easily determined from the numbers of skyrmions observed and the side-lengths of the square lattices chosen for simulations. On the other hand, when no  $E$ -field is applied, 18 FM skyrmions condense to an FM SL in the triangular pattern; as  $E$  is increased to 0.2, the FM SL consisting of 15 elongated skyrmions shows a rotated hexagonal-closely-packed (HCP) structure; while  $E = 0.7$ , the HCP unit cell is twisted, meanwhile the 20 skyrmions are further elongated.

## B. Quantized Topological Charges of Ferroelectric Skyrmions

In continuous models, every magnetic skyrmion can be characterised by an integer number, which is referred to as topological charge, and can be expressed with

$$Q_M = \frac{1}{4\pi} \int \int \mathbf{m} \cdot (\partial_x \mathbf{m} \times \partial_y \mathbf{m}) dx dy, \quad (4)$$

and whose density is given by

$$\rho = \frac{1}{4\pi} \mathbf{m} \cdot (\partial_x \mathbf{m} \times \partial_y \mathbf{m}) . \quad (5)$$

However, our model is discrete and quantized, the topological charges of skyrmions have to be calculated with another set of formulas derived by Berg and his coworker [34]. For a unit square cell with four spins  $\mathbf{S}_1$ ,  $\mathbf{S}_2$ ,  $\mathbf{S}_3$ , and  $\mathbf{S}_4$  at the corners, the topological charge density at the center  $x^*$  is given by

$$\rho(x^*) = \frac{1}{4\pi} [(\sigma A)(\mathbf{S}_1, \mathbf{S}_2, \mathbf{S}_3) + (\sigma A)(\mathbf{S}_1, \mathbf{S}_3, \mathbf{S}_4)] , \quad (6)$$

where  $(\sigma A)(\mathbf{S}_i, \mathbf{S}_j, \mathbf{S}_k)$  stands for the signed area of the spherical triangle with corners  $\mathbf{S}_i, \mathbf{S}_j, \mathbf{S}_k$ , and such a signed area  $(\sigma A)(\mathbf{S}_1, \mathbf{S}_2, \mathbf{S}_3)$  is evaluated with

$$\exp\left[\frac{i}{2}(\sigma A)\right] = \gamma^{-1} [1 + \mathbf{S}_1 \cdot \mathbf{S}_2 + \mathbf{S}_2 \cdot \mathbf{S}_3 + \mathbf{S}_3 \cdot \mathbf{S}_1 + i\mathbf{S}_1 \cdot (\mathbf{S}_2 \times \mathbf{S}_3)] ,$$

$$\gamma = [2(1 + \mathbf{S}_1 \cdot \mathbf{S}_2)(1 + \mathbf{S}_2 \cdot \mathbf{S}_3)(1 + \mathbf{S}_3 \cdot \mathbf{S}_1)]^{1/2} > 0 . \quad (7)$$

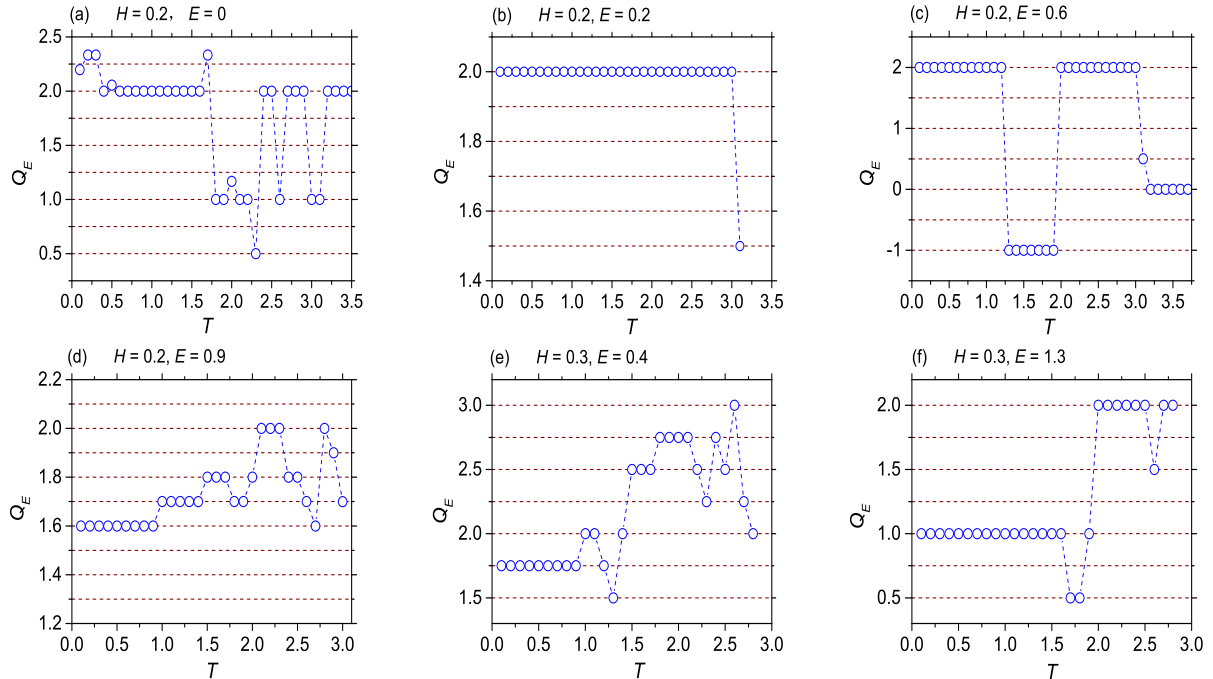


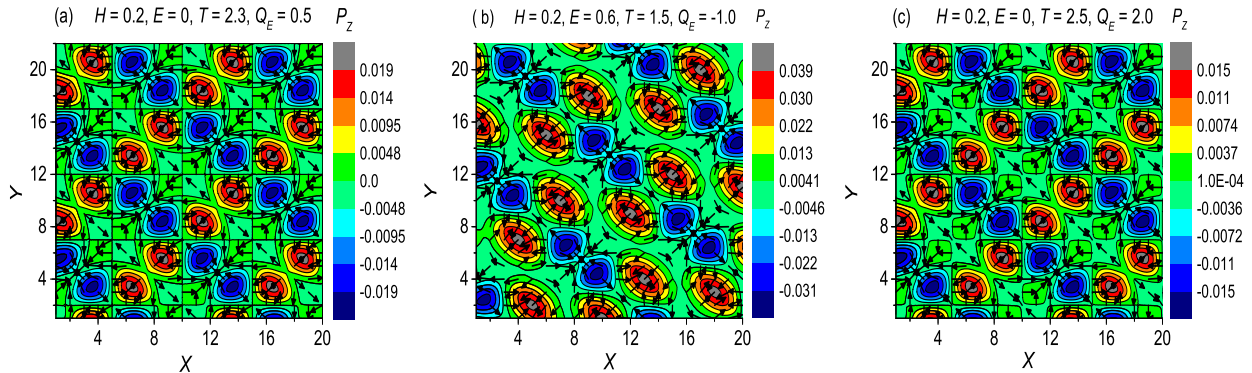
**Figure 3.** Topological charge per skyrmion of the FE SL calculated with (a)  $H = 0.2$ ,  $E = 0$ , (b)  $H = 0.2$ ,  $E = 0.2$ , (c)  $H = 0.2$ ,  $E = 0.6$ , (d)  $H = 0.2$ ,  $E = 0.9$ , (e)  $H = 0.3$ ,  $E = 0.4$ , and (f)  $H = 0.3$ ,  $E = 1.3$ , respectively, versus changing temperature.

Using the above formulas, the topological charge per FM skyrmion,  $Q_M$ , of every FM SL is calculated to be -1.0, though our model is quantized and discrete. Obviously, this set

of formulas can be employed to evaluate the topological charges of FE skyrmions as well. Interestingly, as depicted in Figure 3, most obtained  $Q_E$  values are integers (-1.0, 0, 2.0, 3.0), half integers (0.5, 1.5, 2.5), and odd multiples of 0.25 (1.75, 2.25, 2.75), which form horizontal steps in the curves. More strangely, the allowed  $Q_E$  values can also be 1.6, 1.7, 1.8, 1.9, 2.0, which are the multiples of 0.1, and only when  $E = 0$ ,  $Q_E$  can take other values.

### C. Ferroelectric Skyrmionic Crystals with Z-Contour

Figure 4 displays the FE SLs calculated with and without  $E$ -fields applied. As coupled by ME interaction, FM SL and FE SL appear simultaneously, and every FE skyrmion is formed around an FM skyrmion, so that a pair of FE SL and FM SL contain same number of FE skyrmions and FM skyrmions respectively. Each FE skyrmion is an electric dipole complex consisting of, for example, two red areas (of positive  $P_Z$  values) and two blue regions (of negative  $P_Z$  values), which is a typical feature of the FE skyrmion as calculated by Seki *et al.* though there the FM SLs are the Bloch-type [24]. At first glance, the FE SLs depicted in



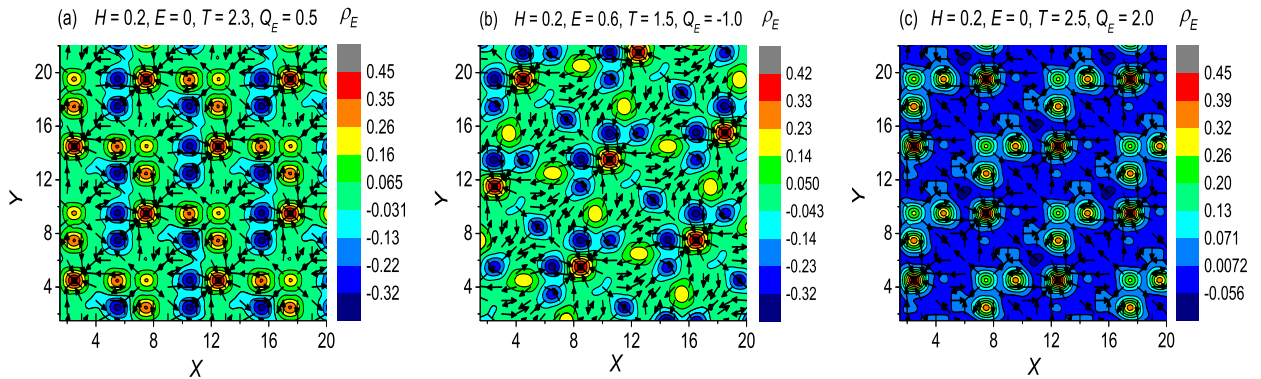
**Figure 4.** FE SL calculated at (a)  $H = 0.2$ ,  $E = 0$ ,  $T = 2.3$ , (b)  $H = 0.2$ ,  $E = 0.6$ ,  $T = 1.5$ , and (c)  $H = 0.2$ ,  $E = 0$ ,  $T = 2.5$ , respectively.

Figure 4(a) and (c) look very similar. However actually, in each FE skyrmion of Figure 4(a), the  $xy$ -components in one blue area are mirror-symmetric to another blue area, but those in the two red regions show no symmetry; whereas in Figure 4(a) and (c), the  $xy$ -components in the blue and red areas of every FE skyrmion are all mirror-symmetric with respect to another corresponding area.

### D. Topological Charge Density Distributions of Ferroelectric Skyrmionic Crystals

The  $\rho_E$  values of every FE SL also form periodic crystal as shown in Figure 5. Since each FE skyrmion is stabilized by an FM skyrmion, and the numbers of the two sorts of

skyrmions observed in a square lattice chosen for simulations are same, it is easy to infer that: in the (a) case, a unit cell of the  $\rho_E$  crystal contains one red, one yellow, two pink and three blue areas; in the (b) case, the unit cell has one red, two yellow and five blue areas; and the last one includes one red, one green and two yellow areas, respectively. These grouped round colored areas appear periodically, though surrounded by much vaster colored background, and the  $\rho_E$  crystals look very distinct from each other. The FE SLs displayed in Figures 4(a) and (c) look very similar. But we see here that the  $\rho_E$  values of most sites are positive in Figures 5(c), so that its averaged topological charge  $Q_E$  takes the largest value.



**Figure 5.** The  $\rho_E$  crystals calculated at (a)  $H = 0.2, E = 0, T = 2.3, Q_E = 0.5$ , (b)  $H = 0.2, E = 0.6, T = 1.5, Q_E = -1.0$ , and (c)  $H = 0.2, E = 0, T = 2.5, Q_E = 2.0$ , respectively.

### E. Three-Dimensional Diagrams of Individual Ferroelectric Skyrmions

Figure 6 displays the three-dimensional (3D) diagrams of the FE skyrmions of  $Q_E = 0.5$ ,

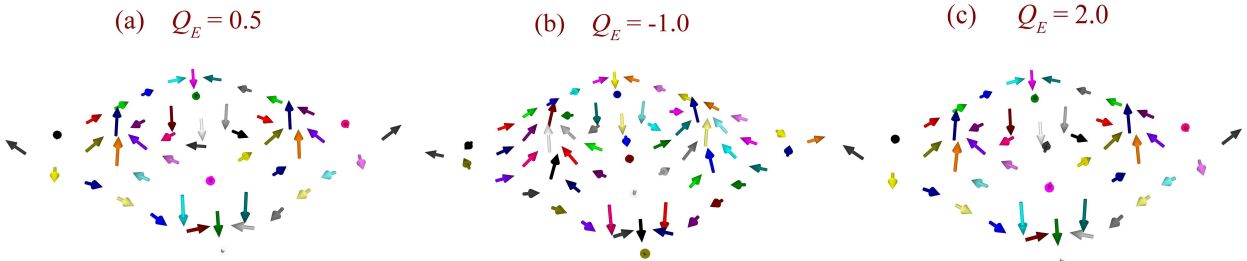


**Figure 6.** Three-dimensional individual FE skyrmions calculated at (a)  $H = 0.2, E = 0, T = 2.3$ , (b)  $H = 0.2, E = 0.6, T = 1.5$ , and (c)  $H = 0.2, E = 0, T = 2.5$ , respectively.

-1.0 and 2.0 respectively. Two peaks (up) and two hollowed (down) areas observed in an FE skyrmion correspond to the red and blue regions depicted in Figure 4. Once again, FE



skyrmion in (b) obviously differ from other two, whereas the two depicted in (a) and (c) look quite similar. However, the  $z$ -components of the FE dipoles in the whole 4-th column with the same  $x$  coordinator are actually different in signs, so that the topological charges are equal to 0.5 and 2.0 respectively in the two cases.

#### IV. CONCLUSIONS AND DISCUSSION

In conclusion, we have calculated and characterized the topological textures of FE SLs formed in a 2D multiferroic monolayer, where DM interaction and ME coupling coexist, by means of a quantum simulating approach. In all cases, the topological charge per FM skyrmion is calculated to be -1.0. On the other hand, an FE SLs is formed once one FM SL is induced, and the topological charges of the FE skyrmions in the FE SLs are usually quantized to be integers, half integers and multiples of certain fractional values. Each FE skyrmion is an electric dipole complex, which is stabilized by one FM skyrmion, so that the FE SL coincides with the FM SL, and the  $\rho_E$  values also form periodic pattern.

As already described above, an normally applied electric fields is able to change skyrmion sizes, and elevate the critical temperature  $T_{SL}$ , that is, to create FM and FE SLs above the original  $T_{SL}$ . On the other hand, we have also found that the FM and FE SLs induced by only external magnetic fields can be destroyed by  $E$ -fields applied afterwards. For example, when  $H = 0.2$  and  $E = 0$ , FM and FE SLs are observed below  $T_{SL} = 3.15$ . If an  $E$ -field of strength 0.6 is considered afterwards and the above calculated results are used as initial configurations to perform simulations, as  $T \in (3.05, 2.5)$ , the FM and FE SLs previously produced disappear, being replaced by FM and FE helical crystals; below that  $T$ -range, the FM and FE SLs are able to maintain their main structures as before, but the FM and FE skyrmions in the crystals are found to be elongated by the  $E$ -field; it is only at  $T = 3.1$ , which is immediately below the original  $T_{SL}$ , that FM and FE SLs of different crystal pattern can be stabilized. In comparison, when both the magnetic and electric fields of the above nonzero strengths are exerted simultaneously, the FM and FE SLs emerge if  $T \leq T_{SL} = 3.17$  as shown in Figure 1(a). These two sets of results are completely different. However, this phenomenon is not strange, since the properties of magnetic systems strongly depend on the magnetizing processes.

The topological chargers of magnetic skyrmions and bimerons are all nonzero integers, and that of a magnetic vortex is equal to 0.5. However here, the FE skyrmions can be characterized by topological numbers of no only integers, half integers, but also the multiples of certain fractional values. This finding is interesting, and may be of importance, the physics behind needs to be further probed in depth.

## Acknowledgements

The author thanks the financial support provided by National Natural Science Foundation of China under grant No. 11274177.

---

- [1] A. N. Bogdanov, and D. A. Yablonskii, *Sov. Phys. JETP*, 95 (1989)
- [2] A. Bogdanov, and A. Huber, *J. Magn. Magn. Mater.* 138, 255-269 (1994)
- [3] B. Binz, A. Vishwanath, V. Aji, *Phys. Rev. Lett.* 96, 207202 (2006).
- [4] S. Muhlbauer, B. Binz, F. Jonietz, C. Pfleiderer, A. Rosch, A. Neubauer, R. Georgii, P. Boni, *Science* 323, 5916 (2009).
- [5] N. Nagaosa, and Y. Tokura, *Nat. Nanotechnol.* 8, 899 (2013).
- [6] A. Fert, V. Cros, and J. Sampaio, *Nat. Nanotechnol.* 8, 152 (2013).
- [7] I. E. Dzyaloshinskii, *Sov. Phys. JETP* 5, 1259 (1957).
- [8] T. Moriya, *Phys. Rev.* 120, 91 (1960).
- [9] A. Fert, and P. M. Levy, *Phys. Rev. Lett.* 44, 1538 (1980).
- [10] A. Fert, *Metallic Multilayers* 59-60, 439 (1990).
- [11] A. Crépieux, and C. Lacroix, *J. Magn. Magn. Mater.* 182, 341 (1998).
- [12] C. Pappas, E. Lelievre-Berna, P. Falus, P. M. Bentley, E. Moskvin, S. Grigoriev, P. Fouquet, and B. Farago, *Phys. Rev. Lett.* 102, 197202 (2009).
- [13] X. Z. Yu, Y. Onose, N. Kanazawa, J. H. Park, J. H. Han, Y. Matsui, N. Nagaosa, and Y. Tokura, *Nature* 465, 901 (2010).
- [14] S. Banerjee, J. Rowland, O. Erten, and M. Randeria, *Phys. Rev. X* 4, 031045 (2014).
- [15] S. D. Yi, S. Onoda, N. Nagaosa, and J. H. Han, *Phys. Rev. B* 80, 054416 (2009).
- [16] S. Buhbrandt, and L. Fritz, *Phys. Rev. B* 88, 195137 (2013).
- [17] S. X. Huang, and C. L. Chien, *Phys. Lett.* 108, 267201 (2012).
- [18] N. Romming, A. Kubetzka, C. Hanneken, K. von Bergmann, and R. Wiesendanger, *Phys. Rev. Lett.* 114, 177203 (2015).
- [19] J. Iwasaki, M. Mochizuki, and N. Nagaosa, *Nat. Commun.* 4, 1463 (2013).
- [20] F. Jonietz, S. Muhlbauer, C. Pfleiderer, A. Neubauer, W. Münzer, A. Bauer, T. Adams, R. Georgii, P. Böni, R. A. Duine, K. Everschor, M. Garst, and A. Rosch, *Science* 330, 1648 (2010).
- [21] T. Schultz, R. Ritz, A. Bauer, M. Halder, M. Wagner, C. Franz, C. Pfleiderer, K. Everschor, M. Garst, and A. Rosch, *Nat. Phys.* 8, 301 (2012).
- [22] K. Everschor, M. Garst, R. A. Duine, and A. Rosch, *Phys. Rev. B* 84, 064401 (2011).
- [23] J. Zang, M. Mostovoy, J. H. Han, and N. Nagaosa, *Phys. Rev. Lett.* 107, 136804 (2011).
- [24] S. Seki, S. Ishiwata, and Y. Tokura, *Phys. Rev. B* 86, 060403 (R) (2012).

- [25] Y. H. Liu, Y. Q. Li, and J. H. Han, *Phys. Rev. B* 87, 100404 (2013).
- [26] Y. H. Liu, J. H. Han, A. A. Omrani, H. M. Ronnow, and Y. Q. Li, arXiv:1310.5293v1 [cond-mat.str-el] 20 Oct 2013
- [27] C. Jia, S. Onoda, N. Nagaosa, and J.H. Han, *Phys. Rev. B* 76, 144424 (2007).
- [28] Y. Tokura, S. Seki, and Y. Tokura, arxiv: 1206.4404v1 (2012).
- [29] Z.-S. Liu, H. Ian, *Superlattices Microstruct.* 138, 106379 (2020) .
- [30] Z.-S. Liu, V. Sechovský, and M. Diviš, *J. Phys.: Condens. Matter* 23, 016002 (2011).
- [31] Z.-S. Liu, V. Sechovský, and M. Diviš, *Phys. Status Solidi B* 249, 202 (2012).
- [32] Z.-S. Liu, and H. Ian, *J. Phys.: Condens. Matter.* 31, 29 (2019).
- [33] Magnetic skyrmion, [https://en.wikipedia.org/wiki/Magnetic\\_skyrmion](https://en.wikipedia.org/wiki/Magnetic_skyrmion)
- [34] B. Berg, M. Lüscher, *Nuclear Phys. B* 190[FS3] , 412 (1981)